Funkcije astrocita u fragilnom X sindromu: in vitro istraživanje

Begić, Darija

Master's thesis / Diplomski rad

2022

Degree Grantor / Ustanova koja je dodijelila akademski / stručni stupanj: **University of Zagreb, Faculty of Food Technology and Biotechnology / Sveučilište u Zagrebu, Prehrambeno-biotehnološki fakultet**

prehrambeno biotehnološki fakultet

zir.nsk.hr

DIGITALNI AKADEMSKI ARHIVI I REPOZITORIJI

University of Orléans - University of Zagreb

Master of Science and Technologies
Specialty: Biotechnologies, Biologie Moléculaire et Cellulaire

INTERNSHIP REPORT

Astroglial function in fragile X syndrome: an *in vitro* investigation

By

Darija Begić

(**February 2022 – June 2022**)

Acknowledgements

Funkcije astrocita u fragilnom X sindromu: *in vitro* istraživanje

Darija Begić, univ. bacc.ing. biotechn, *0058213137*

Sažetak: Fragilni X sindrom (FXS) vodeći je monogenski uzrok poremećaja iz spektra autizma (ASD). Uzrokovan je gubitkom ekspresije FMRP proteina zbog ekspanzije CGG-a. Iako se većina studija usredotočila na uloge FMRP-a u neuronima zbog kognitivnih nedostataka u FXS-u, također se pokazalo da gubitak FMRP-a u astrocitima doprinosi patogenezi FXS-a. Cilj ovog projekta je utvrditi funkcije FMRP-a u astrocitima razvojem strategije prekomjerne ekspresije FMRP-a u astrocitima. U tu svrhu, bila je potrebna karakterizacija astrocita i razvoj učinkovite metode transfekcije. Posebna je pažnja posvećena purinergičkom odgovoru s fokusom na purinergički receptor P2X7. Pokazali smo pojačanu regulaciju purinergičkog odgovora *Fmr1* KO astrocita, posebno u pogledu lučenja interleukina-6 (IL-6) nakon tretmana ATP-om. Najučinkovitija i najfleksibilnija metoda transfekcije je magnetofekcija.

Ključne riječi: *Fragilni X sindrom, FMRP, astrociti, purinergički odgovor, transfekcija*

ASTROGLIAL FUNCTION IN FRAGILE X SYNDROME: AN *IN VITO* INVESTIGATION
Darija Begić, univ. bacc.ing. biotechn.*, 0058213137*

Abstract: Fragile X syndrome (FXS) is the leading monogenic cause of autism spectrum disorders (ASD). It is caused by the CGG expansion-induced loss of fragile X mental retardation protein (FMRP) expression. Although most studies focused on the roles of FMRP in neurons due to cognitive deficits in FXS, the loss of FMRP in astroglia has also been shown to contribute to FXS pathogenesis. The aim of this project is to determine the astrocytic functions of FMRP by developing a strategy to overexpress FMRP in astrocytes. To access that, astrocyte characterization and development of an efficient transfection assay were needed. Particular attention was paid to the purinergic response with a focus on the P2X7 purinergic receptor between the C8-D1A cell line and primary astrocytic cell culture (APC). We demonstrated upregulation of the purinergic response of *Fmr1* KO astrocytes especially regarding interleukin-6 (IL-6) secretion following ATP treatment. The most efficient and flexible transfection method is magnetofection.

Keywords: *Fragile X syndrome, FMRP, astrocytes, purinergic pathways, transfection*

ABSTRACT

Fragile X syndrome (FXS) is the leading monogenic cause of autism spectrum disorders (ASD). It is caused by the CGG expansion-induced loss of fragile X mental retardation protein (FMRP) expression. Although most studies focused on the roles of FMRP in neurons due to cognitive deficits in FXS, the loss of FMRP in astroglia has also been shown to contribute to FXS pathogenesis. The aim of this project is to determine the astrocytic functions of FMRP by developing a strategy to overexpress FMRP in astrocytes. To access that, astrocyte characterization and development of an efficient transfection assay were needed. Particular attention was paid to the purinergic response with a focus on the P2X7 purinergic receptor between the C8-D1A cell line and primary astrocytic cell culture (APC). We demonstrated upregulation of the purinergic response of *Fmr1* KO astrocytes especially regarding interleukin-6 (IL-6) secretion following ATP treatment. The most efficient and flexible transfection method is magnetofection.

Keywords: Fragile X syndrome, FMRP, Astrocytes, Purinergic pathways, P2X7, transfection

RESUME

Le syndrome de l'X fragile (FXS) est la principale cause monogénique de déficience intellectuelle. Elle est causée par une expansion de l'unité CGG au sein du gène FMR1, conduisant à la perte d'expression de la protéine codée FMRP. Bien que la plupart des études se soient concentrées sur les rôles de FMRP dans les neurones, l'expression astrocytaire pourrait également contribuer à la pathogenèse du FXS. La finalité de ce projet est de déterminer les fonctions astrocytaires de FMRP par le développement d'une stratégie de surexpression du FMRP dans les astrocytes. Dans ce contexte, il a été nécessaire au préalable d'établir une caractérisation fonctionnelle in vitro des cultures astrocytaires murines et d'établir une méthode de transfection efficace. Une attention particulière a concerné la réponse purinergique en mettant l'accent sur le récepteur purinergique P2X7 entre la lignée cellulaire C8-D1A et la culture cellulaire primaire astrocytaire (APC). Nous avons démontré une régulation excessive de la réponse purinergique des astrocytes Fmr1 KO en particulier concernant la sécrétion d'interleukine-6 à la suite d'un traitement à l'ATP. La méthode transfection qui s'est révélée la plus efficace et la plus flexible est la magnétofection.

Mots-clés : Syndrome X fragile, FMRP, Astrocytes, Voies purinergiques, P2X7, transfection

Presentation of the Laboratory

The National Center for scientific research (CNRS) is a multidisciplinary public research organization placed under the supervision of the French Ministry of Higher Education, Research, and Innovation. It was founded in 1939 with the role of advancing knowledge for the benefit of society. Its mission consists of five parts: conduct scientific research, transfer research results, share knowledge, train through research, and contribute to scientific policy. It has around 1100 laboratories located through France, mostly Joint Research Units and 36 International Joint Units.

The Laboratory of Molecular and Experimental Immunology and Neurogenetics (INEM) is a part of CNRS located in Orléans. It is the Joint Research Unit (UMR-7355) directed by Valérie Quesniaux that operates in association with the University of Orléans and Regional Hospital Center Orléans. The scientific objectives of the INEM are the study of the molecular and cellular mechanisms involved in host-pathogen relationships, pulmonary inflammation, the genetics of autism and mental deficiencies, and neurotoxicity processes during development. It is divided into two groups: immunology and neuroscience. Immunology consists of two teams: Immune response and Infections and pollutants. Neuroscience consists of two teams: Neurogenetics and Neurotoxicity and development.

I did my internship in the Neurogenetics team led by Dr. Sylvain Briault. Neurogenetics team research genetic and physiopathology of intellectual disabilities (ID) and autistic spectrum disorders (ASD) with emphasis on Fragile X syndrome (FXS).

LIST OF ABREVIATIONS

ACSA-2	Astrocyte cell surface antigen-2
APC	Primary astrocytic cell culture
ATP	Adenosine triphosphate
BSA	Bovine serum albumin
bzATP	2'(3')-O-(4-Benzoylbenzoyl) adenosine 5'-triphosphate triethylammonium salt
DMEM	Dulbecco's Modified Eagle's Medium
DMSO	Dimethyl sulfoxide
ELISA	Enzyme-linked immunosorbent assay
FBS	Fetal bovine serum
FMO	fluorescence minus one
FMR1	Fragile X Mental Retardation 1
FMRP	Fragile X Mental Retardation protein
FXS	Fragile X syndrome
GABA	γ-aminobutyric acid
GFAP	Glial fibrillary acidic protein
GFP	green fluorescent protein
IL	interleukin
KO	Knock-out
LPS	lipopolysaccharide
mEPSC	miniature excitatory postsynaptic current
mGluR	metabotropic glutamate receptor
MTT	3-(4,5-dimethylthiazol-2-yl)-2,5-diphenyltetrazolium bromide
NMDAR	N-methyl-D-aspartate receptor
PBS	Phosphate buffered saline
PFA	Paraformaldehyde
RT	room temperature
SEM	Standard error of the mean
TBS	Tris-buffered saline
TLR	toll like receptor
T-TBS	Tween-tris-buffered saline
WT	Wild type

TABLE OF CONTENTS

LIST OF FIGURES

1.   INTRODUCTION

1.1. Fragile X syndrome

Fragile X syndrome (X) is the common type of X-linked heritable intellectual and autism spectrum disorder (ASD) (Hodges et al., 2017). In more than 99% of cases, it is caused by the expansion of CGG trinucleotide repeats in the 5´ untranslated region of *FMR1* gene, but it can also be caused by mutations in the promoter or coding regions of the gene (Sitzmann et al., 2017). Trinucleotide expansion with more than 200 CGG repeats causes hypermethylation and transcriptional silencing of the gene resulting in the loss of fragile X mental retardation protein (FMRP) (Deng & Klyachko, 2021). Methylation imprint occurs early in embryogenesis, and it is visible as a fragile site (Figure 1) at Xq27.3 or better known as FRAXA site (Willemsen and Kooy, 2017).

Figure 1. Characteristic fragile X site on fragile X chromosome (Willemsen and Kooy, 2017)

FXS affects 1 in 4000 males and 1 in 8000 females (Hatton et al., 2006). Typical phenotype in patients consists of both physical and behavioral manifestations. Physical phenotype is mostly expressed in males and consists of an elongated face, large ears, highly arched palate, macroorchidism, mitral valve prolapse, hyperlaxity of joints, connective tissue dysplasia, and muscular hypotonia. Sometimes typical facial traits may be minimally expressed or lacking altogether, and this phenotype tends to become more noticeable with age (Willemsen and Kooy, 2017). Usually, the only indicators in the newborns are reduced muscle tone, poor suck, and reflux which causes frequent emesis (Hagerman et al., 2017; Willemsen and Kooy, 2017). During the first 3-4 years of life, sleeping problems are particularly expressed (Hagerman et

al., 2017). In females, when the physical traits are present, they usually consist of large ears and an elongated, hypotonic face (Willemsen and Kooy, 2017). Around 20% of individuals with FXS also have epilepsy (Sabaratnam et al., 2001; Deng & Klyachko, 2021). Behavioral manifestations of FXS include anxiety, hyperactivity, attention deficit, emotional lability, gaze avoidance, stereotypic movements, echolalia, and ASD. They are more typical than physical phenotype and can provide better clues for clinical diagnosis (Willemsen and Kooy, 2017). Research showed that 2-6% of individuals with ASD also have an FMR1 mutation and that around 50% of FXS patients have co-occurring autism (Hodges et al., 2020; Smith et al., 2012). Males with FXS have intellectual disabilities, including language delay that can go from borderline normal to severe (Willemsen and Kooy, 2017).

1.2. Fragile X mental retardation protein

FXS is caused by the loss of set of FMRP isoforms. The *FMR1* gene consists of 17 exons and its pre-mRNA transcript is subjected to the alternative splicing (Figure 2). The number of potential produced protein isoforms is very high, but in various tissues, only five to six protein isoforms were detected. Size of detected isoforms is 70 to 80 kilodaltons. Most common isoforms do not contain exon 12 (Bardoni et al., 2001). Dominant mammalian protein isoform has 71 kDa and contains six conserved function domains (Figure 3) (Willemsen and Kooy, 2017).
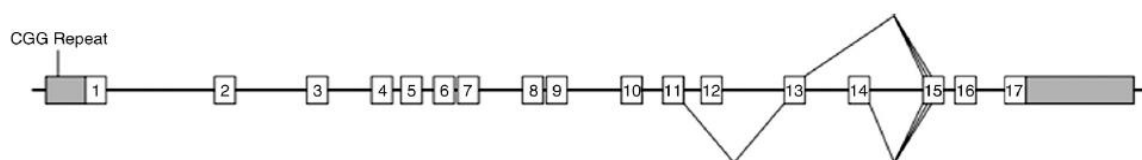
Figure 2. FMR1 splicing pattern and gene structure. (Willemsen and Kooy, 2017).
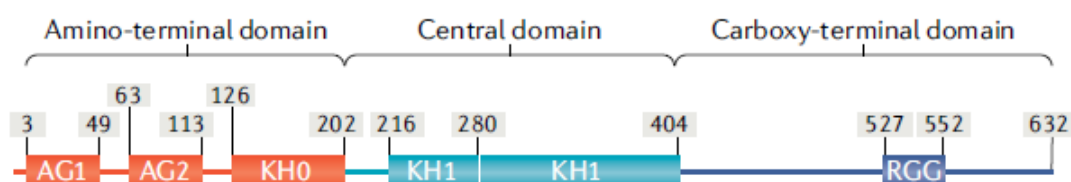
Figure 3. Functional domains of FMRP. Amino-terminal domain consists of two domains involved in protein-protein interactions (AG1 and AG2), nuclear localization signal, and K homology domain (KH0). Central domain contains domains that mediate RNA binding. Carboxy-terminal domain includes a domain that promotes dynamic interactions with proteins and RNAs and the RGG box which is essential for association with polyribosomes (Deng & Klyachko, 2021).

3

Historically, FMRP is known as an mRNA-binding translational repressor. It represses translation by interacting with translation machinery, including microRNA and RNA-binding proteins. Number of potential mRNAs that FMRP binds is high but altered protein levels have been confirmed for only a small percentage of them. In the mouse model, protein screens show a small number of protein changes and many of these may be indirect as they do not align well with mRNA binding data. Recent findings show that FMRP have plenty roles besides being a translational regulator. Just in RNA regulation, it is involved in mRNA editing, pre-mRNA splicing, and the micro-RNA pathway (Davis & Broadie, 2017). FMRP also has a role in genome stabilization as it binds chromatin during the DNA damage response. Furthermore, it is involved in the regulation of cell differentiation, cytoskeleton remodeling, modulation of ion channel functions, neuronal excitability, and synaptic plasticity (Davis & Broadie, 2017; Deng & Klyachko, 2021; De Rubeis et al., 2013).

1.3. Role of FMRP in neurons versus glia

Expression of FMRP is omnipresent, but highest in the CNS and testis (Hagerman et al., 2017; Deng & Klyachko, 2021). In the brain, FMRP binds around 4% of mRNA (Ashley et al., 1993) and it is expressed in neurons, astrocytes, microglia, and oligodendrocytes (Richter & Zhao, 2021; Krasovska & Doering, 2018; Gholizadeh et al., 2015). Due to the focus on cognitive deficits in FXS and the presence of immature dendritic spines as the main morphological alteration in brain, functions of FMRP in neurons received the uppermost attention (Willemsen and Kooy, 2017; Maurin et al., 2014). Association with polyribosomes in soma, axons, and dendritic spines (Darnell et al., 2011; Maurin et al., 2014) and increased expression in response to synaptic activation (Weiler et al., 1997) suggest translational regulation of proteins crucial for proper synaptic function (Darnell et al., 2011) as spine morphology and density are pivotal to synaptic function and connectivity (Hodges et al., 2017). The paramount mechanism for learning disability in FXS is altered synaptic plasticity, in particular, enhanced mGluR5-dependent long-term depression (LTD) in the hippocampus (Jin et al., 2021). Darnell et al. (2011) showed that FMRP represses translation of many plasticity-related and other synaptic proteins by stalling ribosomal translocation. Lack of FMRP promotes mRNA localization to increase growth and presynaptic transmitter release (Davis & Broadie, 2017). One example is increased glutamate release in the axon terminals of dorsal root ganglion neurons (Deng & Klyachko, 2021). FMRP also binds mRNAs which translation does not occur at synapses, and

non-synaptic transcripts (Darnell et al, 2011; Davis & Broadie, 2017). Liao et al. (2008) worked on primary neuron cultures derived from the cortex of Fmr1 KO and WT mice and showed changes in levels of many presynaptic and postsynaptic proteins, including ones that have been associated with autism, mental retardation, epilepsy, or other neuropsychiatric disorders. Aside from altered synaptic transmission and plasticity, dysregulated cellular excitability is present in FXS as neurons exhibit an abnormally high action potential firing rate across different brain regions (Deng & Klyachko, 2021). Part of hyperexcitability in FXS is dysfunction of the GABA system (Jin et al., 2021). Excessive neuronal or circuit excitability could be a reason for sensory hypersensitivity in FXS (Contractor et al., 2015).

Besides roles of FMRP, the main questions in FXS pathophysiology include brain regions and cell types involvement (Jin et al., 2021), especially roles in neurons versus glia (Davis & Broadie, 2017). Historically, glial cells were viewed as secondary cells which provide structural, metabolic, and trophic support to neurons, but they have more active role (Pacey & Doering, 2007). Glial cells play an important part in the regulation of growth, refinement, and function of neuronal circuits, through a number of complex intercellular signaling systems during neurodevelopment (Reynolds et al., 2021a). FXS has been connected with abnormalities of oligodendrocytes and myelination (Dong & Greenough 2004). In oligodendrocytes, FMRP interacts with a subgroup of oligodendrocyte-specific mRNAs, including the myelin basic protein mRNA (Wang et al., 2004). Researches show that astrocytes are important contributors to neurological diseases (Hodges et al., 2017) as they can manage formation, elimination, and maintenance of synapses expressing synaptogenic molecules. These synaptogenic factors are required for normal neuron spine density and morphology during development (Reynolds et al., 2021a). They are involved in various aspects of behavior (Oliveira et al, 2015) and their glycogen breakdown and lactate release are crucial for the formation of long-term memory and maintenance of long-term potentiation (LTP) of synaptic strength (Suzuki et al., 2011). Characterization of FMRP binding mRNAs showed a lot of mRNAs that should be selectively enriched in astrocytes indicating a strong involvement of astrocytes in FXS pathogenesis. Some of these mRNAs are Glul encoding glutamine synthetase, Aldoc encoding aldolase, and Slc1a2 encoding GLT1 (Jin et al., 2021). Higashimori et al. (2016) generated astrocyte-specific Fmr1 conditional knock-out and restoration mice to demonstrate astrocyte-mediated mechanisms in the FXS pathogenesis. They showed that the selective loss of FMRP in astrocytes plays a part in FXS cortical synaptic deficit, probably through dysregulated astroglial glutamate transporter GLT1, which controls extracellular synaptic glutamate levels (Higashimori et al., 2013). Re-

expression of FMRP in astrocyte-specific cON mice completely restores GLT1 expression and glutamate uptake which indicates that astrocyte FMRP has the main role in GLT1 reduction observed in Fmr1 KO mice. Selective loss of astroglial FMRP also contributes to cortical hyperexcitability by increasing NMDAR-mediated evoked, but not spontaneous mEPSCs and elongating cortical UP state duration (Jin et al, 2021). Hodges et al. (2017) created mice in which FMRP can be selectively deleted or exclusively expressed in astrocytes. Their astrocyte specific Fmr1 KO mice showed synaptic and learning defects as well as overproduction of spines during adolescence. Overproduction was not reimbursed by spine pruning and led to behavioral impairments in adulthood. On the other hand, mice that expressed FMRP only in astrocytes also showed spine and learning deficits. That indicates that FMRP expression is necessary in both, neurons and astrocytes and perhaps other cell types for normal brain function.

1.4. Channelopathies caused by lack of FMRP

Channelopathies are disorders caused by the dysfunction of ion channels. They can be result of mutations in genes encoding ion channels or in factors that regulate channels (Deng & Klyachko, 2021). FMRP regulates various channels by either binding them directly or controlling their levels by translational regulation. However, it is unknown if these two types of regulations can be separated (Davis & Broadie, 2017). FMRP deficiency causes different channelopathies, some of which are listed in this report, either by altering their levels, amplitude, gating, or trafficking (El-Hassar et al., 2019). Dysfunctions of different K^+ and Na^+ channels are involved in changes in action potential initiation and firing pattern. In changes of neurotransmitter release, K^+ and Ca^{2+} channels are involved whereas in dendritic function K^+, Ca^{2+}, HCN channels as well as AMPA, NMDA, and $GABA_A$ receptors are involved (Deng & Klyachko, 2021). One of the first described targets of FMRP is mRNA encoding for Kv3.1 potassium channel whose currents are enhanced in fragile X mice (El-Hassar et al., 2019). Other well-known potassium channels involved in FXS are BKCa channels activated by membrane depolarization and increased intracellular Ca^{2+} concentration. They regulate neurotransmitter release and Ca^{2+} concentration in neurons wherefore some autistic and cognitive disorders in FXS can be caused by their abnormalities (Hébert et al., 2014). Voltage gated calcium channels (VGCCs) are also affected in FXS models (Deng & Klyachko, 2021). $Ca_v1.2$, L-type Ca^{2+} channel subunit, is a signal for excitability, long-term plasticity, memory,

and gene expression and its levels are reduced in the human FXS brain (Wang et al., 2014). N-type Ca_v channels – $Ca_v2.2$ have a presynaptic role in the regulation of transmitter release and FMRP controls its surface expression (Ferron et al., 2014). Furthermore, some receptors involved in purinergic signaling are also dysregulated in FXS (Reynolds et al., 2021a).

1.5. Dysregulation of purinergic and immune signaling in FXS

The purinergic signaling system is abundantly expressed in glial and neuronal cell types during crucial developmental periods. It is part of regulatory molecules identified in interactions between astrocytes and neurons (Reynolds et al., 2021a) and it regulates, at least partly, astrocyte-mediated immune signaling (Reynolds et al., 2021b). Purinergic receptors consist of two receptor families, P1 and P2. P1 are receptors for adenosine and P2 are receptors for ATP and its metabolites. Although all P2 receptors work by calcium-dependent mechanisms, they are divided into ionotropic P2X and metabotropic P2Y receptors (Abbracchio et al., 2009). P2X receptors are receptors for purines and P2Y receptors are receptors for purines and pyrimidines (Puchałowicz et al., 2015). These receptors make ATP as an important transmitter and co-transmitter in both the peripheral nervous system and CNS. Nucleotides are released in extracellular space in the physiological state by astrocytes and neurons forming synaptic connections and are important for the proper operating of cells in the nervous system. In large quantities, nucleotides are released after cell damage, mechanical stress, activation, contact with a pathogen, and apoptosis (Puchałowicz et al., 2015). P2X receptors are cationic ligand-operated channels in which pore permeable to potassium, sodium, and calcium opens after binding ATP (Abbracchio et al., 2009). Activation of P2Y receptors stimulates mobilization of intracellular calcium and propagation of calcium into nearby cells which leads to calcium waves and an expanded activated region (Reynolds et al., 2021a). Furthermore, activation of P2Y receptors elevates the expression and release of pro-inflammatory cytokine IL-6 in different cell types (Reynolds et al., 2021b). Elevated IL-6 levels are linked to cognitive impairments, behavioral deficits, decreased social interactions, an increase in formation of excitatory synapse, and a decrease of inhibitory synapse (Krasovska & Doering, 2018). Reynolds et al. (2021a) found greater response to ATP application and enhanced $P2Y_2$ and $P2Y_6$ receptor expression in Fmr1 KO astrocytes in comparison with WT. Hodges et al. (2020) used LPS administration to determine the difference in immune response between Fmr1 KO and WT. LPS is a component of the cell wall of gram-negative bacteria and an agonist of TLR4.

Its administration leads to glial activation and release of pro-inflammatory molecules. Even though glial activation is crucial for neurodevelopment, excessive activation can lead to chronic neuroinflammatory states observed in ASD. Fmr1 KO mice showed significantly elevated IL-6 hippocampal gene expression 4 h after LPS administration. After 24 h IL-6 expression levels were not elevated anymore.

1.5.1 The P2X7 receptor

The P2X7 receptor is a trimeric ATP-gated ion channel that plays an important role in health and disease. It induces inflammatory molecule release, cell proliferation, metabolic events, cell death, and phagocytosis. It can cause excitotoxicity of glial and neural cells by inducing glutamate release. It is activated by a higher concentration of ATP ($\approx$100 µM) than other P2 receptors (Sluyter, 2017). In response to basal or pathological excitation, various cell types secrete ATP and its metabolites in the extracellular space. These molecules bind to purinergic receptors, including P2X7 (Reynolds et al., 2021a). After binding ATP, P2X7 opens pores for the rapid flux of potassium, sodium, calcium, and other small cations. It can also open large pores for some organic ions and fluorescent dyes such as etidium$^+$ after prolonged ATP stimulation (Sluyter, 2017; Bartlett et al., 2014). Downstream signaling pathways after P2X7 activation lead to the secretion of inflammatory mediators, such as IL-1β, IL-18, and consequently IL-6, IL-8, and TNF-α (De Marchi et al., 2016). Besides ATP and its metabolites, P2X7 can be activated by the synthetic ATP analog, bzATP, and intracellular LPS which can induce IL-6 expression (Sluyter, 2017; Van Snick, 1990). Interestingly, the P2X7 receptor-mediated signaling was described in glia cells, including astrocytes and microglia and should be involved in several neuropathological processes.

1.6. Objective

The main objective of this project is to explore the consequences of *Fmr1* overexpression in astrocytes with the focus on purinergic pathways and comparison of IL-6 secretion in *Fmr1* KO and WT followed by activation of purinergic receptors. Within this project, the internship had two main goals. The first goal was the characterization of C8-D1A cell line and astrocytes primary cell cultures (APC). C8-D1A clonal permanent cell line with the morphology of fibrous astrocytes was established from explant cultures of 8-day postnatal mouse cerebellum (Alliot F & Pessac B, 1984). APC were established from the cortex of 1-5 days old *Fmr1* KO and WT pups. Cell characterization involved the examination of cell identities, ATP response,

and IL-6 secretion. In addition, previous preliminary experiment performed in the laboratory by De Concini V. suggested defect of expression of P2X7 in *Fmr1* KO by flow cytometry (preliminary results, data not shown). This internship had a task to explore this genotype effect in APC purinergic activities.

The second goal of this internship was to determine the best transfection method and the best transfection conditions for both, C8-D1A cell line and APC.

2. MATERIALS AND METHODS

2.1. C8D1A cell line

C8-D1A cell line [Astrocyte type I clone] was purchased from American Type Culture Collection, cultured in DMEM, high glucose (Sigma Aldrich) supplemented with 10% heat-inactivated fetal bovine serum (RB35956, HyClone), 1% Penicillin/Streptomycin (P4333, Sigma Aldrich) and 1% L-glutamine (59202C, Sigma Aldrich) and incubated at 37°C and 5% CO_2. This clonal permanent cell line with the morphology of fibrous astrocytes was established from explant cultures of 8-day postnatal mouse cerebellum, strain C57BL/6 (URL1). For passaging, cells were washed 3 times with PBS (Sigma Aldrich) and incubated with 0.25% trypsin/EDTA solution (25200-056, Gibco) for 3 min. Trypsin was inactivated by adding a complete medium and solution was centrifuged at 110 g at 4°C for 5 min. The supernatant was thrown and cells were resuspended and seeded in the new medium.

2.2. Isolation and culturing of astrocytes-rich primary cell cultures

Cells were isolated from Fmr1 WT and Fmr1 KO mice at P1 to P5. Genotype of pups was determined using reverse (S6R: 5´-ATT CTT CTG GCA CCT CCA GC-3´) and forward primers (S7F: 5´-TGT GAT AGA ATA TGC AGC ATG TGA-3´, M3F: 5´CAC GAG ACT AGT GAG ACG TG-3´) following the supplier´s instructions (KK5151, Sigma-Aldrich, Missouri, USA). The brain was placed in a petri dish containing phosphate-buffered saline. Under binocular loupe the olfactory bulbs and cerebellum were removed, two hemispheres were separated by cutting on both sides of the septum and the striatum, and the meninges were removed. Dissected hemispheres were placed in 2 ml of Dulbecco's Modified Eagle's Medium, high glucose (Sigma Aldrich) supplemented with 10% heat-inactivated fetal bovine serum, 1% Penicillin/Streptomycin, and 1% L-glutamine. Cells were dissociated mechanically with a P1000 pipette and centrifugated for 5 min at 110 g and 4°C. The supernatant was removed and cells were dissociated in a new complete medium. Cells were seeded at a density of 80 000 cells per well in 24 wells plates. Cultures were incubated at 37°C and 5% CO_2. Every 2-3 days plates were shaken at 200 rpm for 40 min prior to changing the medium to enrich culture in astrocytes.

2.3. Enzyme-linked immunosorbent assay (ELISA)

Astrocytes-rich primary cell cultures and C8-D1A cell cultures were stimulated with LPS (1µg/µl; L2630, Sigma Aldrich), ATP (200 µM and 500 µM; A2383, Sigma Aldrich), bzATP (200 µM; 5.05734.0001, EMD Millipore Corp., USA) and P2X7 antagonist (10 µM, 50 µM, and 200 µM; A 74003, Bio-techne). After 4, 8, and 24 hours post-treatment medium was taken and stored at - 20°C. The release of interleukin-6 (IL-6) was determined by the ELISA assay kit (Mouse IL-6, DuoSet®, R&D Systems) according to the manufacturer's instructions. Absorbance was measured at 450 nm by the EL×800™ NB Microplate reader (BioTek® Instruments).

2.4. MTT assay

Astrocytes-rich primary cell cultures and C8-D1A cell cultures were treated with ATP (200 µM), bzATP (200 µM), and P2X7 inhibitor (10 µM and 50 µM). After 6h of incubation at 37°C and 5% CO_2, the medium was taken for ELISA and 10% MTT (M5655, Sigma Aldrich) diluted in a new medium (DMEM, high glucose) was added (200 µl/well). Plates were incubated for 2 h at 37°C and 5% CO_2 after which the DMSO (Sigma Aldrich) was added (500 µl/well) to solubilize the formazan crystals. To get homogeneous solutions whose color is measurable with a spectrophotometer, plates were shaken for 15 min. Absorbance was measured at 570 nm by the CLARIO Star Microplate reader (BMG LABTECH).

2.5. Transfection assays

Transfection assays were performed when cells reached 50-70% of confluence. Transfection was observed after 24 h with fluorescent microscopy and flow cytometry, and after 3 days with fluorescence microscopy.

2.5.1. ESCORT™ IV transfection reagent
Plasmids solutions were prepared by adding 1 µg of plasmid in 100 µl of DMEM, high glucose medium supplemented with 1% of L-glutamine for one well. ESCORT IV (L3287, Sigma Aldrich) solutions were prepared by adding 3 µg of transfection reagent in 100 µl of DMEM, high glucose medium supplemented with 1% of L-glutamine for one well. Plasmids solutions were added to ESCORT IV solutions and mixed gently by pipetting liquid up and down.

Complexes were left at RT for ≈45 min. Meanwhile, cells were washed two times with DMEM, high glucose medium supplemented with 1% of L-glutamine. For 24 wells plate, 200 µl of DNA/liposome complex solution per well was added in a dropwise manner and mixed by gently swirling the plate. Plates were incubated for 4-6 h (37°C, 5% of CO_2) and the medium used for transfection was changed with complete supplemented DMEM, high glucose medium to restore normal serum and antibiotic concentration. Cells were incubated overnight (37°C, 5% of CO_2).

2.5.2. PTG1 transfection reagent

Plasmids solutions were prepared by adding 1 µg of plasmid DNA per well in a final amount of 40 µl of 10mM Hepes, pH 7.4. The polymer solutions were prepared by adding 4.5, 6 or 7.5 µg of PTG1 (Polytheragene) per well to an equivalent volume of Hepes. Polymer solution was added drop by drop on DNA, vortexed, and incubated for a minimum of 30 min at RT. Solution volume was adjusted to 500 µl per well with opti-MEM medium (Gibco) and added drop by drop on cells. Plates were incubated for 4 h before changing medium with DMEM, high glucose supplemented medium.

2.5.3. Lip100

Plasmids solutions were prepared by adding 1 µg of plasmid DNA per well in a final amount of 40 µl of Hepes. Lip100 (Perche et al., 2011) was diluted in a final amount of 200 µl of Hepes and incubated at RT for 15 min. Lip100 solution was added drop by drop on DNA solutions, mixed by gentle pipetting, and incubated at RT for 15 min. Solution volume was adjusted to 500 µl per well with opti-MEM medium. Plates were incubated for 4 h before changing medium with DMEM, high glucose supplemented medium. Ratio 1:2 of DNA: Lip100 was tested.

2.5.4. Lipopolyplexes

Plasmids solutions were prepared by adding 1 µg of plasmid DNA in a final amount of 40 µl of Hepes. For polymer solution, 3 µg of PTG1 were added to 3 µl of Hepes. The polymer was added drop by drop on DNA, vortexed, and incubated for a minimum of 30 min at RT. Lip100 (2 µg) was diluted in a final amount of 200 µl of Hepes and incubated for 15 min at RT. Lip100 was added drop by drop on polyplexes with delicate pipetting and the solution was incubated for 15 min at RT. The volume of the lipopolyplexes solution was adjusted to 500 µl of opti-MEM medium per well. Plates were incubated for 4 h before changing medium with DMEM, high glucose supplemented medium.

2.5.5. NeuroMag

Magnetofection with NeuroMag reagent (NM50500, OZ Biosciences) was performed following the manufacturer's protocol. For the preparation of DNA: NeuroMag complexes DMEM, high glucose medium was used. Ratios 1:1, 1:2 and1:3 of DNA to NeuroMag product were tested.

2.6. Plasmid DNA

For all transfection assays, PLO3-p3NF-cmv-eGFP-3NF (REFERENCE?) which encodes for green fluorescence protein, and p-EGFP-C1-Flag-mFmr1 (87929, Addgene) which encodes for a GFP fused with FMRP, were used. Both plasmids are driven by CMV ubiquitous strong promoter. Plasmids were isolated from *Escherichia coli* with maxiprep kit (Qiagen) following the instructions. Transfection efficiency was evaluated using flow cytometry, western blot, and/or fluorescence microscopy.

2.7. Flow cytometry

Cells were washed three times with PBS and detached with 100 µl of trypsin-EDTA solution 24 h post-transfection. For the first experiment, cells were transferred to 500 µl of complete medium and centrifuged for 5 min at 220 g. The supernatant was taken, the pellet was resuspended in 300 µl of PBS, and stored on ice. Right before flow cytometry, 1 µl of propidium iodide (1 mg/ml) was added per 100 µl of a sample, and vortexed. Data was recorded with a BD Fortessa x20 flow cytometer (Becton Dickinson, USA). For every other experiment, after trypsinization, cells were transferred to 96 wells plate with 100 µl of complete medium with the serum to inactivate trypsin. The plate was centrifuged at 300g and 4°C for 10 min. Supernatant was removed, and cells resuspended in 200 µl of FACS medium (PBS + EDTA, 2 mM + FBS, 2%). The plate was centrifuged again at 300g and 4°C for 10 min. Supernatant was removed and cells were stained with extra-cellular antibodies: Fixable Viability Dye (eBiosciences[TM], 65-0865-14, 1/800), anti-ACSA-2-APC (Miltenyi Biotec, 130-117-535, 1/50), anti-CD45 V450 (BD Horizon[TM], 560501, 1/100), anti-CD11b PerCP-Cy[TM]5.5 (BD Pharmingen[TM], 550993, 1/100) and blocked with non-conjugated anti-CD16/32 (BD Pharmingen[TM], 553142, 1/100) for 20 min in the dark at RT. C8-D1A cells were not stained with anti-CD45 V450 and anti-CD11b PerCP-Cy[TM]5.5. Once again, plate was centrifuged at

300g and 4°C for 10 min after which the pellet was resuspended in 200 µl of FACS Lysing (10X BD FACS™ Lysing Solution diluted in reagent grade water) and stored in the dark at 4°C. Data were recorded with a flow cytometer (BD FACSCanto™ II, BD Biosciences). For adjusting parameters non-stained and mono-stained controls with beads (Invitrogen) were used. One drop of beads was diluted in 200 µl of PBS and 1 µl of antibody was added. Instead of GFP, FITC anti-CD86 antibody (BD Pharmingen™, 553691) was used, and APC-Cy™7 anti-CD8a antibody (BD Pharmingen™, 557654) was used instead of Fixable Viability Dye. Data were analyzed with FlowJo software V10 (tree Star, Ashland, OR), and compensation was done using FMO controls. For analysis cells were gated on SSC-A FSC-A graphs, single cells on FSC-A FSC-H graphs, live cells on FSC-A L/D graphs, astrocytes on FSC-A ACSA2$^+$ graphs, microglia on CD45$^+$CD11b$^+$ graphs (only for primary cell cultures) and transfected cells on FSC-A GFP$^+$ graphs.

2.8. Western Blot

Cells were rinsed three times with PBS and lysed with 1X RIPA lysis buffer (89901, Thermo Scientific, Massachusetts, USA) containing 1X Protease Inhibitor Cocktail (78429, Thermo Scientific, Massachusetts, USA) followed by sonication for 3min. Protein concentrations were quantified using Pierce™ BCA Protein Assay Kit (23227, Thermo Scientific, Massachusetts, USA) following the manufacturer's instructions. Absorption was measured at 562 nm with a CLARIO Star Microplate reader (BMG LABTECH), and samples were stored at -20°C. Before electrophoresis samples were defrosted, mixed with reducing agent β-mercaptoethanol, and incubated at 95°C for 5 min. Proteins (21 µg per sample) were loaded on 4% stacking and 10% running polyacrylamide gel, run at 100V until reaching running gel, and at 160V for 1.5h. For monitoring protein migration during SDS electrophoresis, protein transfer, and determining the size of proteins pre-stained protein ladder (26616, PageRuler™ 10-180 kDa, Thermo Scientific, Massachusetts, USA) was used. After electrophoresis, proteins were transferred to a nitrocellulose membrane using a semi-dry transfer cell (TRANS-BLOT® SD, BioRad, California, USA) at 200 mA for 40 min. Membranes were washed three times with 1X T-TBS and blocked with 1X T-TBS containing 5% non-fat milk for 2 h at RT. After blocking, membranes were incubated with primary antibodies diluted in 1X T-TBS containing 5% non-fat milk overnight at 4°C. Used primary antibodies are anti-GFP (Abcam ab290, 1/2000) and anti-β-actin (Sigma A2228, 1/6000). After 5 rinses with 1X T-TBS membranes were incubated

for 1h at RT with secondary antibodies diluted in 1X T-TBS containing 5% non-fat milk and then rinsed 5 times with 1X T-TBS before detection. As secondary antibody anti-rabbit-IgG-HRP-linked (Promega W4011, 1/4000) or anti-mouse-IgG-HRP-linked (Promega W4021, 1/4000) were used. Blots were revealed using ECL Western Blotting Detection Reagents (RPN2209, Amersham^{TM}) or SuperSignal^{TM} West Femto reagent (34094, Thermo Scientific^{TM}) and captured with Western blot imager Pxi4 (Syngen, Ozyme, France).

2.9. Immunocytochemistry

Cells were washed three times with PBS (Sigma Aldrich) and fixed with PFA 4% for 10 min on RT 24 h post-transfection. After fixation cells were washed three times with 1X TBS. Coverslips were retrieved from the bottoms of plate´s wells and placed on the support. They were incubated with 100 µl of blocking solution for primary antibodies (1X TBS, 0.2% Triton, 1% BSA, 10% FBS, and 1% Azide) for at least 15 min. Next, coverslips were drained and incubated with 100 µl of blocking solution for primary antibody with the diluted primary antibody for 2h at RT or overnight at 4°C. As primary antibodies, anti-GFAP (Dako 20334, 1/500), and anti-P2X7 (Alomone Apr 004, 1/100) were used. Incubation with primary antibody was followed by draining coverslips and washing them in 1X TBS three times. Then, coverslips were incubated with 100 µl of blocking solution for secondary antibody (1X TBS, 1% BSA, 10% FBS, 1% Azide) with diluted secondary antibody (Anti-Rabbit IgG H&L, Abcam ab6792, 1/100) for 1 h at RT. To avoid free fluorochrome aggregates, prior to incubation solution of secondary antibody was centrifugated at 5000 g for 5 min. After incubation, coverslips were drained and washed three times in 1X TBS, incubated with 100 µl of DAPI solution for 1 min, drained, washed three times in 1X TBS, and washed once in distilled water. Coverslips were mounted with a drop of Fluoromount-G$^{®}$ mounting medium (0100-01, SouthernBiotech) and stored at 4°C. Observation of fluorescence was done with a fluorescent microscope (Leica DM6000B, Leica Biosystems, Germany) and recorded with a camera (C14440, ORCA-fusion, Hamamatsu) using Metamorph$^{®}$ software. Pictures were analyzed with Image J.

2.10. Statistical

For data analysis, GraphPad Prism v9 (GraphPad Software) was used. Errors were reported as standard error of the mean (SEM). Statistical significance was determined with One-way ANOVA or Two-way ANOVA followed by Tukey post-test. As statistically significant, P values ≤0.05 were considered.

3. RESULTS

3.1. Purinergic response in astrocytes

Besides providing structural, metabolic, and trophic support to neurons, glial cells have more active role in CNS. Astrocytes play an important part in neuroinflammatory response, including the release of many cytokines. The purinergic signaling system, which is activated by nucleotides and especially ATP, is involved in astrocyte-mediated immune signaling and cytokine release. Moreover, it is essential as ATP serves both as alarmin and mediator released by neurons.

That being the case, in this project astrocytes were treated with ATP for 24 h and IL-6 release was analyzed 4, 8, and 24 h post-treatment to determine the kinetic of IL-6 secretion (Figure 4, Figure 5a). As a positive control, LPS treatment was used (Figure 4, Figure 5b). In basal conditions, IL-6 secretion is very low, for both C8-D1A cell line and APC. C8-D1A cell line had a fast response on ATP treatment with significantly elevated IL-6 release 4 h post-treatment. From 4 to 8 h IL-6 release was slightly elevated and was steady from 8 to 24 h. On the other hand, IL-6 release following LPS treatment was not fast, but it significantly increased over time.
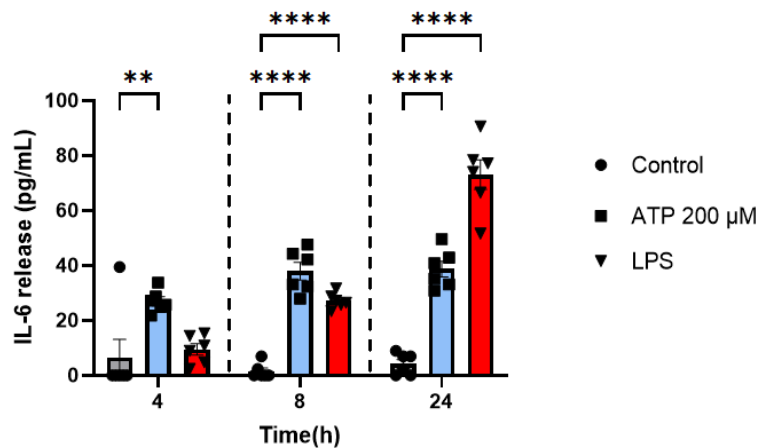
Figure 4. Kinetic of IL-6 release following ATP and LPS treatment in C8-D1A cell line.
C8-D1A cell line was treated with ATP and LPS for 24 h and the medium was picked 4, 8, and 24 h post-treatment to determine the concentration (pg/mL) of released IL-6 with ELISA. Data are expressed as mean ± SEM, n = 6 per condition. Two-way ANOVA followed by a Tukey *post hoc* test was used for statistical analysis. **$p \leq 0.01$, ****$p \leq 0.0001$.

There was no significant genotype effect between *Fmr1* KO and WT in IL-6 release in basal conditions of IL-6 release. 4 h post-treatment there was no significant elevation in IL-6 release after ATP nor LPS treatment. Once again, IL-6 release from 8 to 24 h followed by ATP treatment was steady. Also, IL-6 secretion followed by LPS stimulation increased significantly. Both ATP and LPS treatment induced significantly higher secretion of this cytokine in *Fmr1* KO compared to *Fmr1* WT astrocytes.
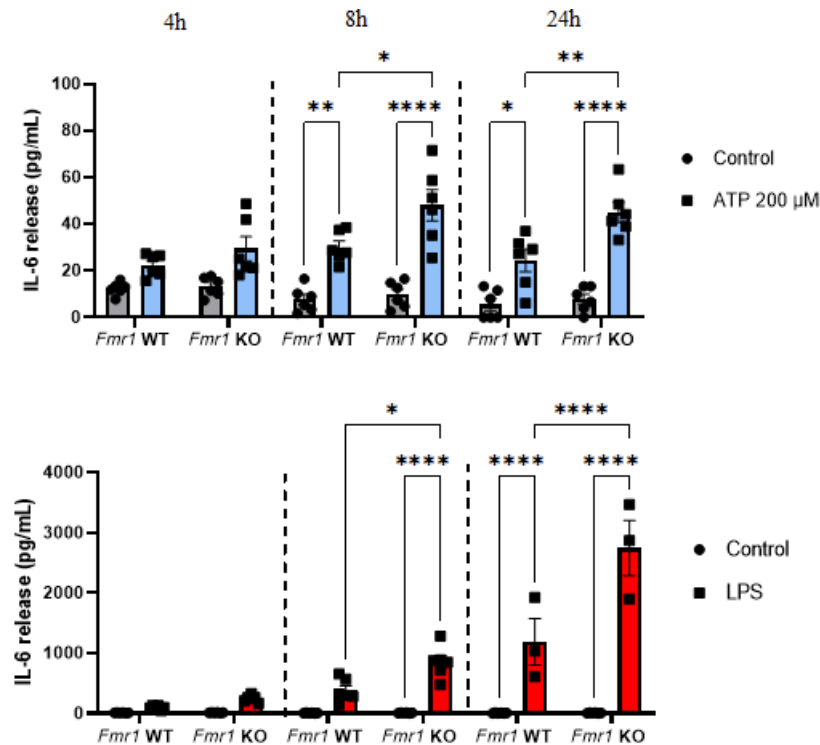
Figure 5. Kinetic of IL-6 release following ATP and LPS treatment in *Fmr1* WT and KO APC.
Fmr1 WT and KO APC were treated with ATP (a) and LPS (b) for 24 h and the medium was picked 4, 8, and 24 h post-treatment to determine the concentration (pg/mL) of released IL-6 with ELISA. Data are expressed as mean ± SEM, n = 6 per condition. Two-way ANOVA followed by a Tukey *post hoc* test was used for statistical analysis. *$p \leq 0.05$, **$p \leq 0.01$, ****$p \leq 0.0001$.

P2X7 purinergic receptor pathway is extensively involved in cytokine secretion, wherefore astrocytes were treated with a solution of ATP and different concentrations of P2X7 specific antagonist – A740003 (Figure 6a, Figure 7), and bzATP (Figure 6b, Figure 7), Again, IL-6 release in C8-D1A and APC in the basal condition is very low or undetectable. After 24 h of treatment in C8-D1A cell line all three solutions with ATP and different concentrations of A740003 induced significantly less secretion of IL-6 than treatment with ATP alone. Concentrations of released IL-6 in wells treated with the highest concentration of antagonist were even not detectable. As before, after 6 h, treatment with ATP induced elevated IL-6

release. Stimulation with bzATP also induced significantly (p = 0.0402) raised IL-6 release, although lower than ATP (p = 0.0004). Treatment with bzATP and A740003 showed lower, even though not statistically significant, cytokine secretion than treatment with only bzATP.
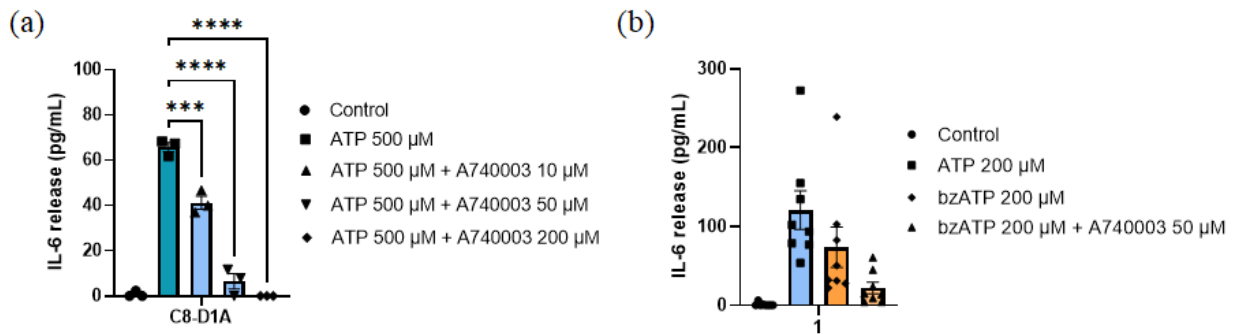
Figure 6. IL-6 release in C8-D1A followed by treatment with P2X7 specific antagonist and activator.
C8-D1A cell line was treated with ATP, and A740003 for 24 h (a) and with ATP, bzATP and A740003 for 6 h (b). The medium was picked, and IL-6 concentration (pg/mL) was measured by ELISA. Data are expressed as mean ± SEM, n = 3 (a) or n = 8 (b) per condition. One-way ANOVA followed by Tukey *post hoc* test was used for statistical analysis. ***p ≤ 0.001, ****p ≤ 0.0001.

One more time, after 24 h of stimulation with ATP *Fmr1* KO showed significantly greater (p = 0.0024) IL-6 secretion than *Fmr1* KO. Both genotypes had a decrease in cytokine secretion with the addition of P2X7 antagonist and even non-detectable concentration of IL-6 release after treatment with the highest concentration of antagonist. Besides that, they had a higher response to bzATP than ATP and this response was similar between genotypes. In addition, both genotypes had a similar and significant decrease in cytokine release with solution of antagonist and bzATP.
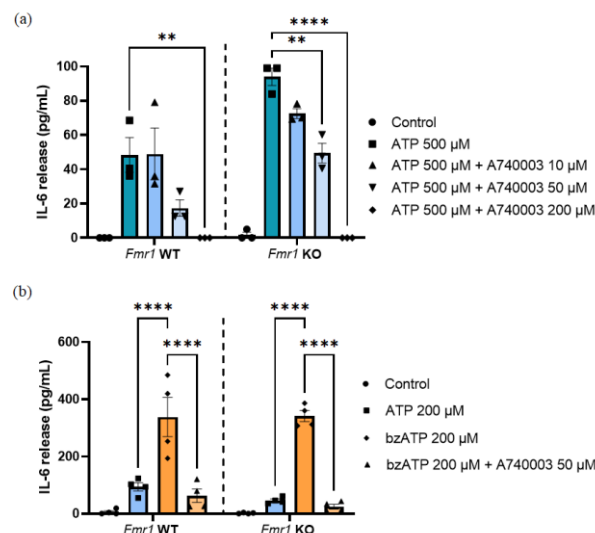
Figure 7. IL-6 release in *Fmr1* KO and WT APC followed by treatment with P2X7 specific antagonist and activator.
Fmr1 WT and KO APC were treated with ATP and A740003 for 24 h (a) and with ATP, bzATP, and A740003 for 6 h (b). The medium was picked, and IL-6 concentration (pg/mL) was measured by ELISA. Data are expressed as mean ± SEM, n = 3 (a) or n = 4 (b) per condition. Two-way ANOVA followed by Tukey *post hoc* test was used for statistical analysis. **p ≤ 0.01, ****p ≤ 0.0001.

In all experiments, astrocytes had a lower response when P2X7 antagonist was added. To exclude A740003 cytotoxicity as the reason, an MTT assay was performed (Figure 8, Figure 9). C8-D1A cell line and APC, regardless of genotype, had elevated % of related cytotoxicity followed by treatment with A740003. Treatments with ATP and bzATP did not show any significant cytotoxic effect on either cell type.
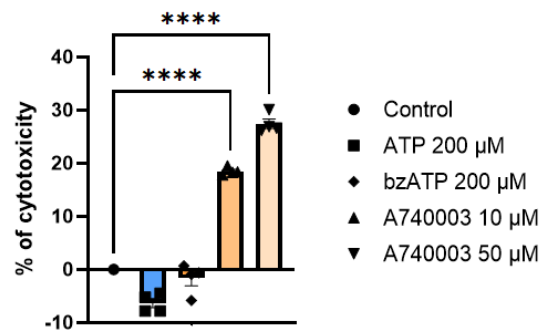
Figure 8. Cytotoxic effect of ATP, bzATP, and A740003 on C8-D1A cells.
C8-D1A cell line was treated with ATP, bzATP, and A740003 for 6 h after which an MTT assay was performed. Data are expressed as mean ± SEM, n = 4 per condition. One-way ANOVA followed by Tukey *post hoc* test was used for statistical analysis. ****$p \leq 0.0001$.
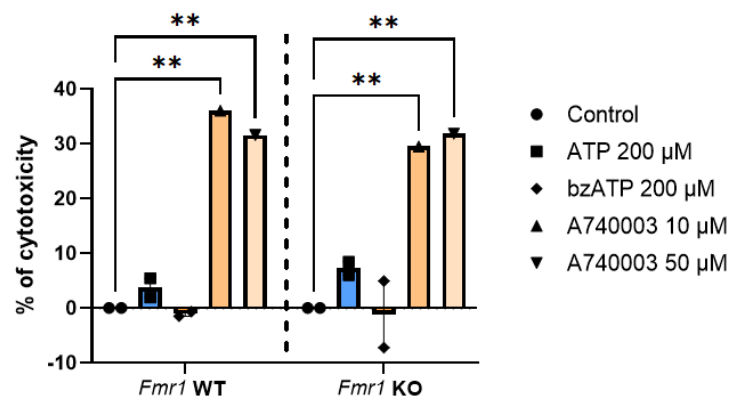
Figure 9. Cytotoxic effect of ATP, bzATP, and A740003 on *Fmr1* KO and WT APC.
Fmr1 KO and WT APC were treated with ATP, bzATP, and A740003 for 6 h after which an MTT assay was performed. Every dot represents the mean of three wells. Data are expressed as mean ± SEM. Two-way ANOVA followed by Tukey *post hoc* test was used for statistical analysis. **$p \leq 0.01$. ,

On the other hand, just an observation of ATP, bzATP, and A740003 cytotoxic effect on C8-D1A cell line (Figure 10) did not show a clear cytotoxic effect of A740003. As MTT assay showed similar results for C8-D1A and APC, these observations probably extend to APC as well.
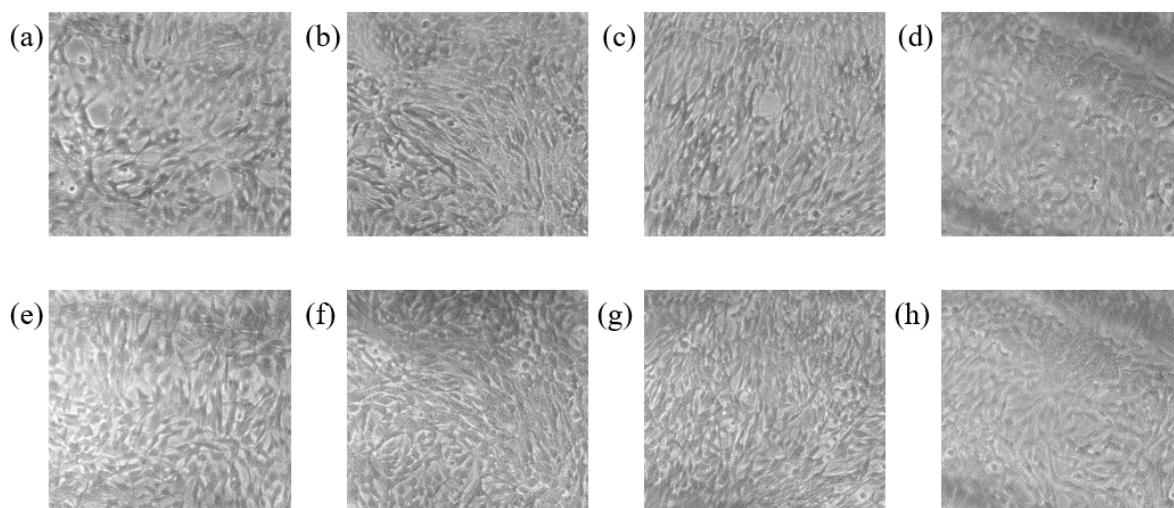
Figure 10. Observations of ATP, bzATP, and A740003 *effects* on *confluence of* C8-D1A cell line. C8-D1A cell line was treated with ATP, bzATP, and A740003 for 6 h. Pictures were taken right before [(a) control, (b) 200 µM ATP, (c) 200 µM bzATP, (d) 50 µM A740003] and right after treatment [(e) control, (f) 200 µM ATP, (g) 200 µM bzATP, (h) 50 µM A740003].

3.2. Transfection assays

To determine the consequences of Fmr1 overexpression in astrocytes it was necessary to develop the best transfection strategy. A good transfection strategy would mean low toxicity and great efficacy which is manifested as a high percentage of transfected cells. Toxicity and efficacy of transfection assays were determined by flow cytometry. The first experiment on C8-D1A cell line (Figure 11) showed the highest transfection efficiency with ESCORT IV transfection reagent with a plasmid coding for GFP. Transfection with lipopolyplexes had lowest transfection efficiency of all methods. Transfection efficiency with a plasmid coding for FMRP-GFP fusion protein was similar for ESCORT IV and PTG1 transfection reagents and higher than one with Lip100 transfection reagent. Transfection with lipopolyplexes and Lip100 transfection reagent had the highest toxicity with both plasmids, while transfection with PTG1 transfection reagent had the lowest toxicity with both plasmids. These results were the reason for excluding lipopolyplexes and Lip100 transfection reagent from other experiments.
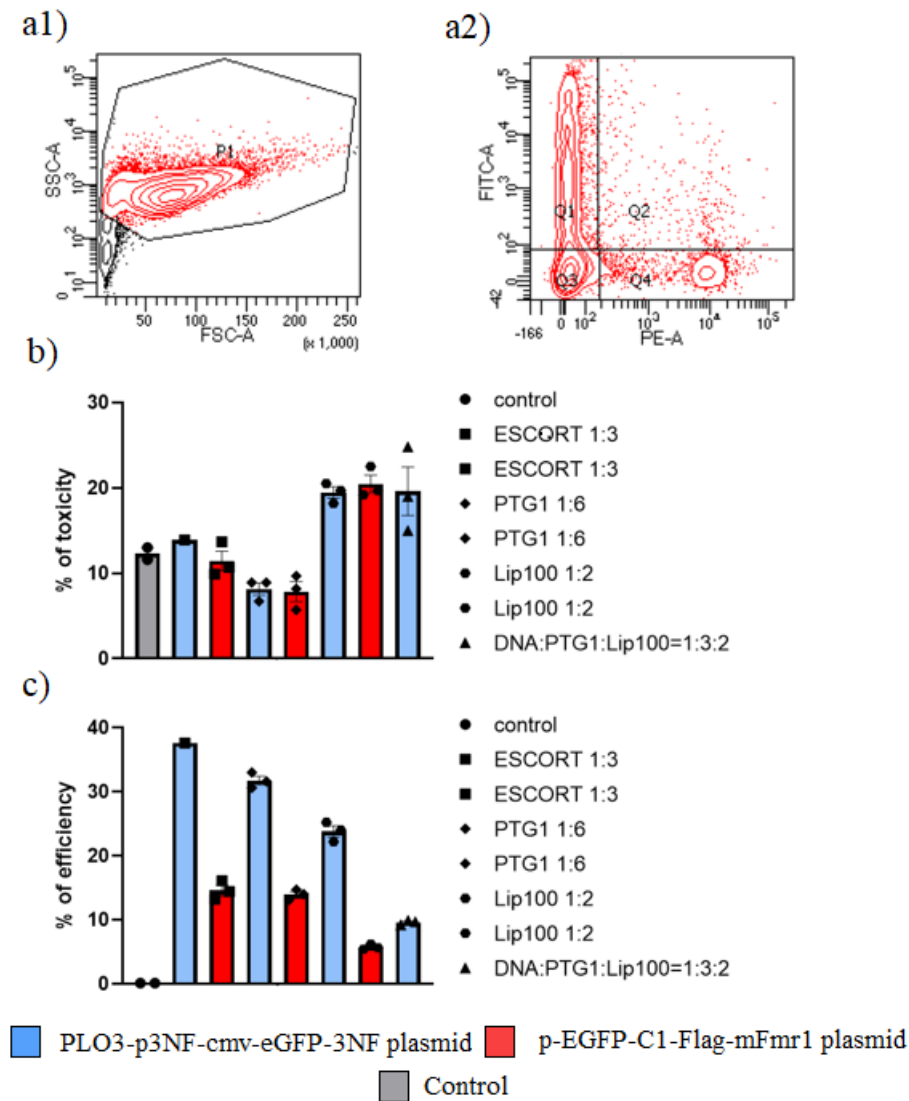
Figure 11. Toxicity and efficiency of transfection assays in C8-D1A cell line
C8-D1A cell line was transfected with a plasmid coding for GFP or FMRP-GFP with different transfection methods. 24 h post-transfection cells were detached with trypsin and mixed with propidium iodide to determine the percentage of transfected and percentage of dead cells by flow cytometry. An example of gating shows gating of cells (a1) and gating of transfected and dead cells (a2) where Q2 and Q4 represent dead cells - toxicity (b) while Q1 represents alive and transfected cells - efficiency (c).

Other transfection experiments on C8-D1A cell line were used not just for determining toxicity and efficiency of transfection assays, but also for cell characterization. An example of gating for flow cytometry (Figure 12b) shows that the majority of C8-D1A cells express ACSA-2. Taking into consideration just transfection of cells that express ACSA-2 (Figure 12a), the best transfection efficiency with a plasmid coding for GFP showed NeuroMag transfection reagent in 1:2 ratio, although transfection efficiency with PTG1 transfection reagent in both ratios was not lower. Best transfection efficiency with a plasmid coding for FMRP-GFP fusion protein

was with PTG1 transfection reagent in 1:4.5. Toxicities of all transfection assays in this experiment were similar (data not shown). All these data are preliminary results with a limited number of samples and must be statistically confirmed.

Figure 12. The efficiency of different transfection assays in C8-D1A expressing ACSA-2.
C8-D1A cell line was transfected with a plasmid coding for GFP or Fmr1-GFP with different transfection methods. 24 h post-transfection cells were detached with trypsin and immunostained with anti-ACSA-2 antibody to determine if these cells express ACSA-2 and with fixable viability dye. Data analysis was done in FlowJo software V10 and transfection efficiency was determined for cells that express ACSA-2 (a). An example of gating (b) is shown on a sample transfected with PTG1 and plasmid coding for GFP, in 1:4.5 ratio.

To verify transfection efficiency and control GFP and FMRP-GFP expression, transfection assays followed by western blot and immunocytochemistry were done. GFP protein was detected by western blot (Figure 13) in samples transfected with a plasmid coding for GFP. FMRP-GFP protein was not detected in this experiment. The reason could hide in transfection efficiency quantified by flow cytometry which is significantly lower (p<0.0001) than one with a plasmid coding for GFP, resulting in a lower concentration of FMRP-GFP than GFP on the membrane.
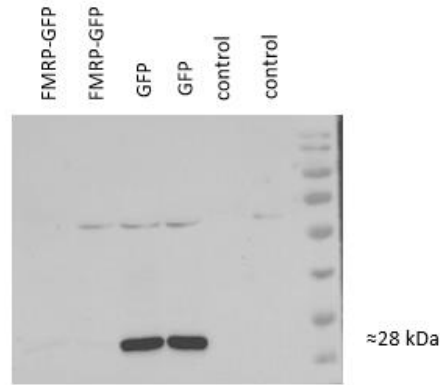
Figure 13. Western blot of GFP performed on proteins isolated from transfected C8-D1A cells.
C8-D1A cell line was transfected with plasmids coding for GFP and FMRP-GFP fusion protein and NeuroMag product in 1:2 ratio. 24-h post-transfection proteins were isolated and quantified. 21 µg of proteins were added per well. The membrane was revealed using ECL detection reagent.

Immunocytochemistry (Figure 14, Figure 15) was not done only for verifying transfection efficiency and localization of GFP and FMRP-GFP expression within cells, but also for broadening cell characterization. Immunocytochemistry results confirmed successful transfection with both plasmids, but with low efficiency. It is visible that GFP is localized throughout the whole cell, while FMRP-GFP fusion protein is localized in dots. Taking into consideration that FMRP is broadly known as a translational repressor, this cell distribution should be associated within polyribosomal complex. Furthermore, these results showed that C8-D1A cells express GFAP and P2X7.
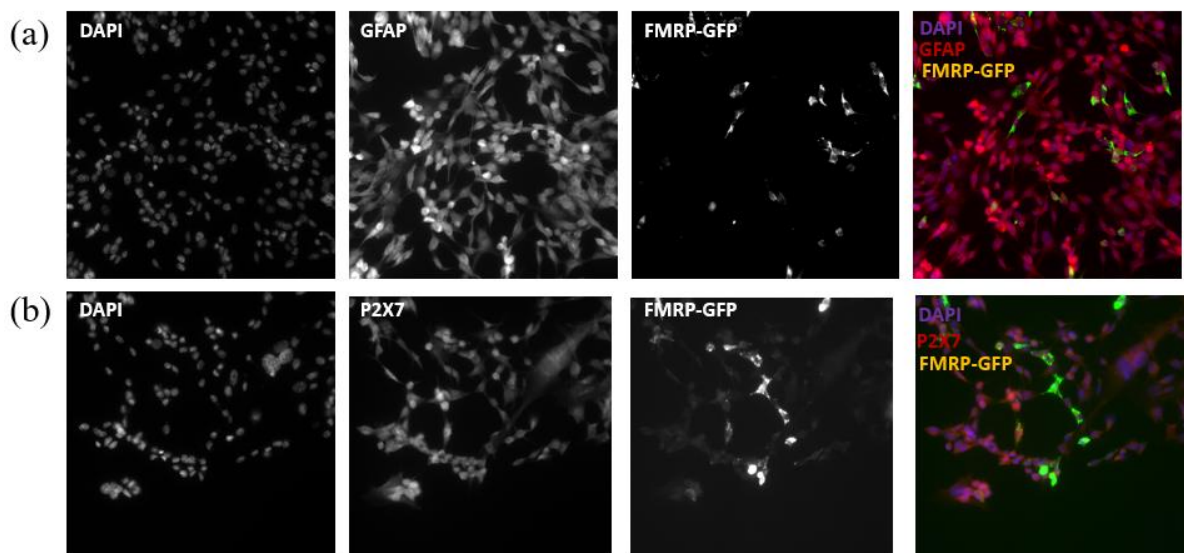

Figure 14. Example of merging photos in ImageJ software.
Pictures were taken with a fluorescent microscope and analyzed with ImageJ software. In this figure examples of merging photos in ImageJ, for C8-D1A cells transfected with a plasmid coding for GFP and GFAP (a) and P2X7 (b) staining, are shown.
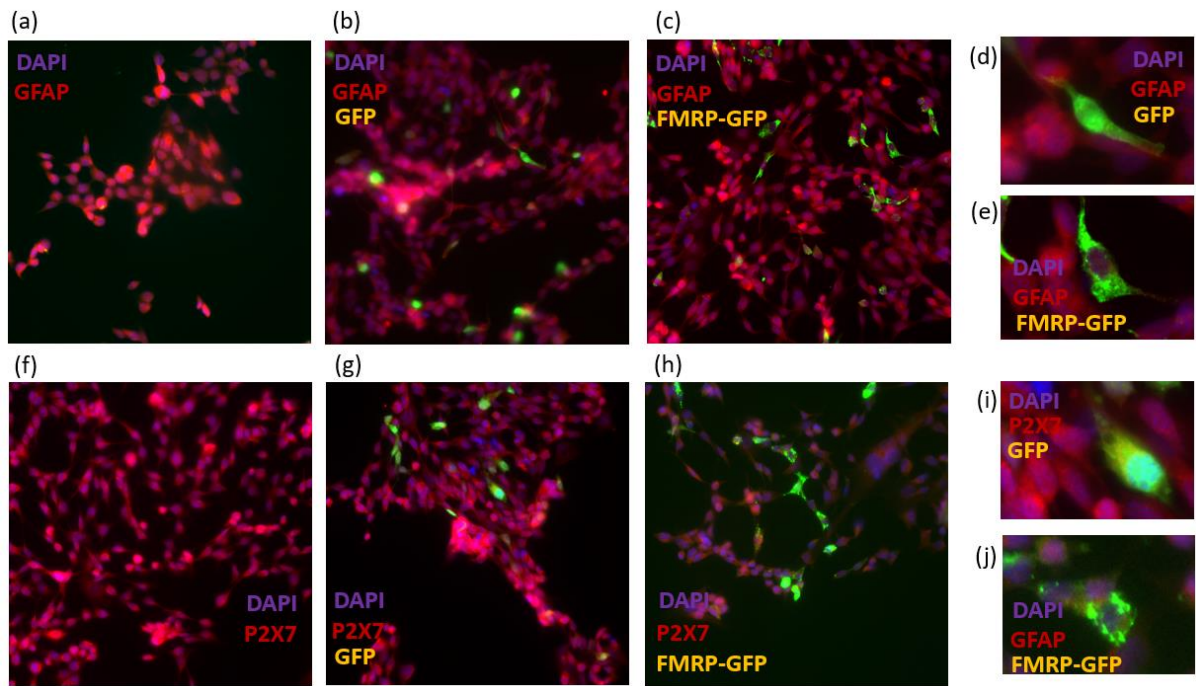
Figure 15. GFAP and P2X7 staining of C8-D1A transfected cells.
24 h post-transfection with ESCORT IV transfection reagent (ratio 1:3), GFAP (a, b, c, d, e), and P2X7 staining (f, g, h, i, j) were performed to determine the expression of these proteins in C8-D1A cells. In control (a, f) there is no GFP fluorescence. In samples transfected with a plasmid coding for GFP (b, g) there is visible GFP fluorescence as well as in samples transfected with a plasmid coding for FMRP-GFP fusion protein. Localization of GFP (d, i) and FMRP-GFP (e, j) is clearly visible.

APC were transfected to determine the best transfection assay for these cells and see if it is different from one for C8-D1A cells. Transfection efficiency with a plasmid coding for FMRP-GFP (Figure 16a) was highest with NeuroMag transfection method and lowest with ESCORT IV transfection reagent (only the best ratios for each method are shown in the figure). The toxicities of used transfection assays are very similar (data not shown). An example of gating (Figure 16b) shows that the majority of cells in APC are astrocytes expressing ACSA-2. It also shows that APC contain only a small percentage of microglia cells. Successful transfection was verified with Western blot (Figure 17). FMRP-GFP fusion protein was detected in samples transfected with ESCORT IV transfection reagent and p-EGFP-C1-Flag-mFmr1 plasmid. Non-specific bands around 37 kDa were detected. GFP was detected but the overexposed signal linked to its high concentration was not shown.
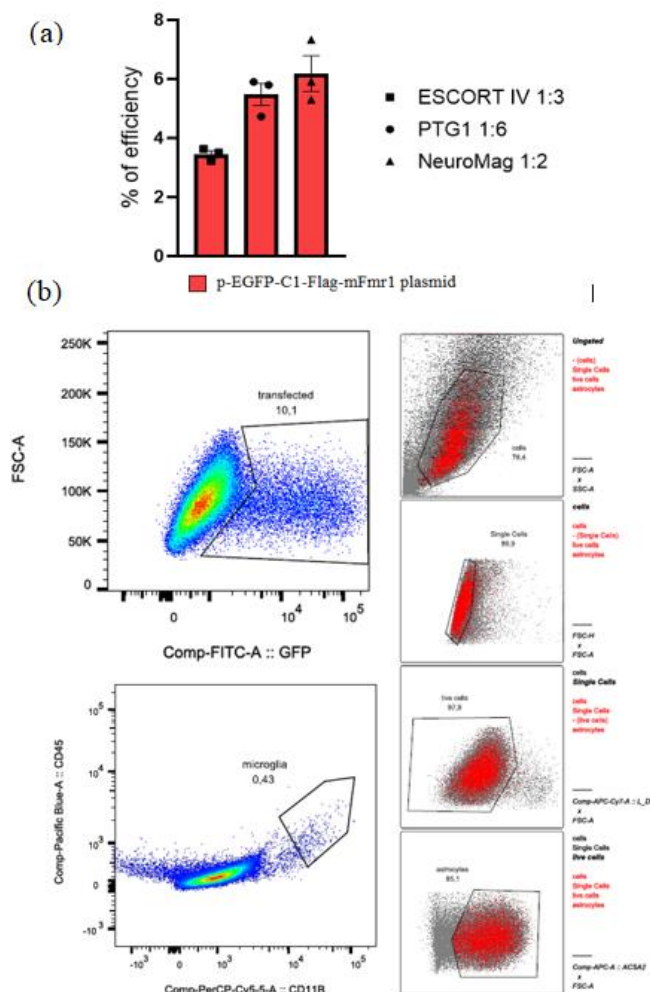
Figure 16. The efficiency of different transfection assays in *Fmr1* WT APC.
Fmr1 WT APC was transfected with a plasmid coding for FMRP-GFP fusion protein with different transfection methods. 24 h post-transfection cells were detached with trypsin and immunostained with anti-ACSA-2, anti-CD45, and anti-CD11B antibodies to determine the percentage of astrocytes and microglia and with fixable viability dye to exclude dead cells. Data analysis was done in FlowJo software V10 and transfection efficiency was determined for cells that express ACSA-2 (a). An example of gating (b) is shown on a sample transfected with NeuroMag.

Figure 17. FMRP-GFP detected by western blot after transfection.
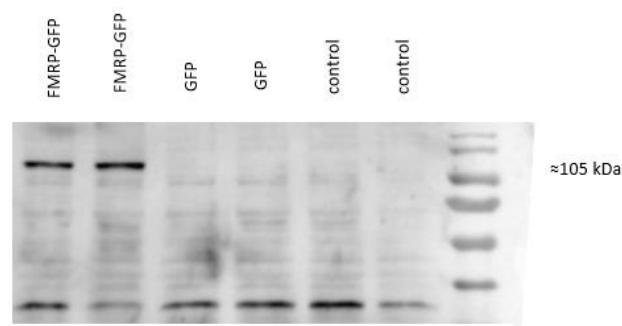Fmr1 WT APC was transfected with plasmids coding for FMRP-GFP fusion protein and ESCORT IV transfection reagent. 24-h post-transfection proteins were isolated and quantified. 21 µg of proteins were added per well. The membrane was revealed using SuperSignal™ West Femto reagent.

26

4. DISCUSSION AND CONCLUSIONS

Fragile X syndrome is the most common monogenic cause of intellectual deficiency (McLennan et al., 2011). One of the main questions concerning FXS pathophysiology refers to the involvement of brain regions and cell types (Jin et al., 2021). To date, most studies on FXS were focused on the roles of FMRP in neurons (Maurin et al., 2014). That being the case, the purpose of this project is to explore the FMRP functions in astrocytes using a *Fmr1* overexpression strategy. Since the expression defect of P2X7 in *Fmr1* KO mice was detected within the team (De Concini, unpublished results), the project´s focus is on purinergic pathways and this receptor. Before determining the consequences of *Fmr1* overexpression, characterization of astrocytes that are going to be used in the project was needed as well as the development of a good transfection assay that will enable *Fmr1* overexpression.

In this project, two types of astrocyte cultures were used, cell line and primary culture. C8-D1A is an astrocyte clonal cell line established from 8-day old mouse cerebellum. Astrocyte primary cultures were established from the cortex of 1-5 days old *Fmr1* KO and WT mice. As observed by flow cytometry the APC contained up to 2% of microglia.

Both cultures secrete proinflammatory cytokine IL-6 after ATP and LPS treatment. Although the kinetic of IL-6 release is similar, APC secrete much more IL-6 following LPS treatment than C8-D1A. The reason for that could hide in difference between cultures as C8-D1A are astrocytes from the cerebellum and APC are astrocytes derived from the cortex. Moreover, as a cell line, C8-D1A probably consists of the same population of astrocytes while APC contains several astrocytes populations and a low percentage of microglia.

Besides the difference in response between cultures, we observed a genotype effect in APC. *Fmr1* KO had elevated IL-6 release after treatment with ATP and LPS. This heightened response of *Fmr1* KO is supported by previous published data. Indeed, Hodges et al. (2020) showed elevated IL-6 expression 4 h post-LPS administration in *Fmr1* KO mice. Aside from that paper, Krasovska & Doering (2018) demonstrated increased IL-6 levels in the *Fmr1* KO cortex and astrocytes.

ATP is a crucial mediator in interactions between astrocytes and between astrocytes and other cell types in the brain. ATP release can activate different receptors, including purinergic receptors which signaling is a key in neuron-glia and glia-glia interactions (Nikolic et al., 2019). Reynolds et al. (2021a) connected lack of FMRP with purinergic upregulation as they demonstrated elevated expression of $P2Y_2$ and $P2Y_6$ purinergic receptors in *Fmr1* KO mice.

They also detected elevated intracellular calcium mobilization and thrombospondin-1 secretion in *Fmr1* KO mice followed by P2Y receptor activation with ATP and UTP. To investigate other purinergic pathways in FXS, our team focused on P2X receptors and suggest an expression defect of P2X7 in *Fmr1* KO mice (De Concini, unpublished results). To broaden research about P2X7 receptor, astrocytes were treated with bzATP which is P2X7 specific activator, and A740003 which is P2X7 specific antagonist. These results indicate that both cultures express P2X7 and could indicate several levels of P2X7 expression between cultures. Treatment with ATP and even the lowest concentration of A740003 significantly decreased IL-6 secretion in comparison to treatment with only ATP in C8-D1A cell line. On the other hand, that concentration of inhibitor did not decrease IL-6 secretion in *Fmr1* WT. It is visible that the addition of an inhibitor decreases IL-6 secretion in C8-D1A to a greater extent than in APC. Even though there is no high percentage of microglia in APC, they could be a reason for this difference. Microglia cells can be activated by ATP, and they are one of the main sources of pro-inflammatory factors in the CNS, including IL-6. Furthermore, microglia and astrocytes probably show synergistic effect in neuroinflammatory response (Yang & Zhou 2019). Besides microglia, cell confluence could be an additional reason, as experiments on C8-D1A were done with lower confluence than ones on APC. Regarding only APC, both genotypes had a decrease in cytokine secretion, but *Fmr1* KO had a significant decrease with a lower concentration of inhibitor. These results may confirm previously observed expression defect of P2X7 in *Fmr1* KO mice in the lab (De Concini, unpublished results). C8-D1A cells and APC, regardless of genotype, secreted IL-6 after bzATP treatment which confirms that they express P2X7 receptor. There is no difference in response of *Fmr1* KO and WT to bzATP treatment, but it does not necessarily mean no difference in P2X7 receptor expression and function. The half maximal effective concentration of bzATP is about tenfold lower than the concentration required for ATP which goes from ≈50 µM (Sluyter, 2017). Used bzATP concentration (200 µM) could be too high to show any genotype effect. It would be good to test the genotype effect with lower bzATP concentrations in the future.

For claiming that reason for cytokine decrease after inhibitor treatment is P2X7 expression and not just cytotoxicity of inhibitor itself, it is mandatory to exclude it. For this reason, MTT assay was performed. It showed elevated cytotoxicity after A740003 treatment. MTT assay is based on the reduction of water-soluble tetrazolium salt MTT to colored formazan. The reduction is usually assigned to mitochondrial enzymes and electron carriers, but in mammalian cells, it is also catalyzed by several nonmitochondrial enzymes (Bernas & Dobrucki 2002). It has been recently discovered that P2X7 receptor also localizes to mitochondria and that is a key

modulator of mitochondrial energy metabolism (Sarti et al., 2021). That being the case, MTT assay may not be the best method to determine the cytotoxicity of P2X7 antagonist. In the future, another method for determining cytotoxicity, that does not involve mitochondrial activity, is needed. That method could be lactate dehydrogenase assay. It is another colorimetric method for determining cytotoxicity. Lactate dehydrogenase is cytosolic enzyme that is released from dead cells and its release is measured by a coupled enzymatic reactions (Aslantürk, 2018). For now, observations under a microscope did not show a cytotoxic effect.

The second goal of this internship was to develop a good transfection assay with great efficiency and low toxicity as a good transfection method is mandatory for FMRP overexpression. Our first results on C8-D1A cells showed the highest transfection efficiency with ESCORT IV transfection reagent and the lowest with lipopolyplexes. As transfections with lipopolyplexes and Lip100 had the highest toxicity these transfection methods were excluded from further experiments. If a comparison between the first and second experiments is made, a decrease in transfection efficiency is visible. For the second experiment, only ACSA-2 positive cells were considered in transfection efficiency and that could be a part of the reason for the decrease. Other parts could hide in a different confluence of cells as the confluence is a very important condition for good transfection. Considering the second experiment on C8-D1A cell line, transfection efficiency with a plasmid coding for GFP was the best with NeuroMag transfection reagent, although it was not excessively lower with PTG1 or ESCORT IV. Transfection with a plasmid coding for FMRP-GFP fusion protein was best with PTG1, but not significantly. Transfection of *Fmr1* WT with p-EGFP-C1-Flag-mFmr1 was best with NeuroMag transfection reagent. Moreover, we were able to observe GFP expression two weeks after transfection with NeuroMag, while with ESCORT IV it was observed for one week (data not shown). As all three methods had similar toxicity, and Neuromag had the highest efficiency in most experiments (data not shown), we chose NeuroMag as the best method. Furthermore, magnetofection with NeuroMag product is easier and more flexible than other tested methods. NeuroMag method will become the standard transfection method in the lab for the continuation of this project. In the future, efficiency could be better with determining the best transfection conditions such as the best confluence, ratio of NeuroMag and plasmid DNA, and time of transfection.

Addressing flow cytometry experiments, it is also relevant to emphasize that ASCA-2 has been shown as a good marker for C8-D1A cell line as it can not be found in the literature.

Besides flow cytometry, our project focuses on immunocytochemistry and western blot as additional methods for determining successful transfection. Immunocytochemistry also enables determining the localization of expressed GFP and FMRP-GFP fusion protein. Our results show that GFP is localized throughout the whole cell, while FMRP-GFP fusion protein is localized in dots. It has been demonstrated that FMRP is associated with polyribosomes in the mammalian brain (Stefani et al., 2004) which could mean that the visible doted localization of FMRP-GFP is a sub ribosomal localization. In the future, this could be explored using staining with anti-ribosomal antibody. This kind of localization also suggests that GFP tag did not disturb FMRP function. In project continuation, this method could be the main method for the detection of FMRP-GFP overexpression. Besides, it can be used if additional characterizations of cells will be needed. For now, we confirmed that C8-D1A expresss GFAP and P2X7.

GFP and FMRP-GFP were detected by western blot. GFP was detected with ECL detection reagent, however, FMRP-GFP was not. Detected transfection efficiency was significantly lower for transfection with a plasmid coding for FMRP-GFP than with a plasmid coding for GFP and resulted in a lower concentration of FMRP-GFP on the membrane. As that concentration was too low for detection with ECL reagent, detection with a more sensitive reagent that allows detection of lower protein levels was attempted. It enabled detection of FMRP-GFP, but with a high background. Finding good conditions for western blot is valuable for the project as it would allow determining changes in FMRP-GFP expression after ATP, bzATP, and A740003 treatment in both cultures.

Based on method developed in this internship, mRNA targets of FMRP in astrocytes should be defined. Indeed, recently Men et al. (2022) discovered that lack of FMRP alters the subcellular localization and expression of process-localized mRNAs and determined potential mRNAs regulated by FMRP in cortical astroglia.

In the future, this project could help in discovering mRNA targets of FMRP in astrocytes. After transfection with a plasmid coding for FMRP-GFP, transfected cells could be isolated by fluorescence-activated cell sorting and RNAs in interactions with FMRP by RNA immunoprecipitation. Transcriptomic examination could be done by comparison to cells transfected with a plasmid coding for GFP. These future experiments could be done on C8-D1A and *Fmr1* KO and WT APC to compare different astrocyte cultures and different genotypes.

5. REFERENCES

1. Abbracchio, M. P., Burnstock, G., Verkhratsky, A., & Zimmermann, H. (2009). Purinergic signalling in the nervous system: an overview. *Trends in neurosciences*, *32*(1), 19-29.

2. Alliot, F. & Pessac, B. (1984). Astrocytic cell clones derived from established cultures of 8-day postnatal mouse cerebella. Brain Res. 306: 283-291.

3. Ashley Jr, C. T., Wilkinson, K. D., Reines, D., & Warren, S. T. (1993). FMR1 protein: conserved RNP family domains and selective RNA binding. *Science*, *262*(5133), 563-566.

4. Aslantürk, Ö. S. (2018). In vitro cytotoxicity and cell viability assays: principles, advantages, and disadvantages. *Genotoxicity-A predictable risk to our actual world*, *2*, 64-80

5. Bardoni, B., Schenck, A., & Mandel, J. L. (2001). The Fragile X mental retardation protein. *Brain research bulletin*, *56*(3-4), 375-382.

6. Bartlett, R., Stokes, L., & Sluyter, R. (2014). The P2X7 receptor channel: recent developments and the use of P2X7 antagonists in models of disease. Pharmacological reviews, 66(3), 638-675.

7. Bernas, T., & Dobrucki, J. (2002). Mitochondrial and nonmitochondrial reduction of MTT: Interaction of MTT with TMRE, JC-1, and NAO mitochondrial fluorescent probes. *Cytometry: The Journal of the International Society for Analytical Cytology*, *47*(4), 236-242.

8. Contractor, A., Klyachko, V. A., & Portera-Cailliau, C. (2015). Altered neuronal and circuit excitability in fragile X syndrome. Neuron, 87(4), 699-715.

9. Darnell, J. C., Van Driesche, S. J., Zhang, C., Hung, K. Y. S., Mele, A., Fraser, C. E., Stone, E. F., Chen, C., Fak, J. J., Chi, S. W., Licatalosi, D. D., Richter, J. D., & Darnell, R. B. (2011). FMRP stalls ribosomal translocation on mRNAs linked to synaptic function and autism. *Cell*, *146*(2), 247-261.

10. Davis, J. K., & Broadie, K. (2017). Multifarious functions of the fragile X mental retardation protein. *Trends in Genetics*, *33*(10), 703-714.

11. De Marchi, E., Orioli, E., Dal Ben, D., & Adinolfi, E. (2016). P2X7 receptor as a therapeutic target. Advances in protein chemistry and structural biology, 104, 39-79.

12. De Rubeis, S., Pasciuto, E., Li, K. W., Fernández, E., Di Marino, D., Buzzi, A., Ostroff, L. E., Klann, E., Zwartkruis, F. J. T., Komiyama, N. H., Grant, S. G. N., Poujoul, C., Choquet, D., Achsel, T., Posthuma, D., Smith, A. B. & Bagni, C. (2013). CYFIP1 coordinates mRNA translation and cytoskeleton remodeling to ensure proper dendritic spine formation. *Neuron*, *79*(6), 1169-1182.

13. Deng, P. Y., & Klyachko, V. A. (2021). Channelopathies in fragile X syndrome. *Nature Reviews Neuroscience*, *22*(5), 275-289.

14. Dong, W. K., & Greenough, W. T. (2004). Plasticity of nonneuronal brain tissue: roles in developmental disorders. Mental retardation and developmental disabilities research reviews, 10(2), 85-90.

15. El-Hassar, L., Song, L., Tan, W. J., Large, C. H., Alvaro, G., Santos-Sacchi, J., & Kaczmarek, L. K. (2019). Modulators of Kv3 potassium channels rescue the auditory function of fragile X mice. Journal of Neuroscience, 39(24), 4797-4813.

16. Ferron, L., Nieto-Rostro, M., Cassidy, J. S., & Dolphin, A. C. (2014). Fragile X mental retardation protein controls synaptic vesicle exocytosis by modulating N-type calcium channel density. Nature communications, 5(1), 1-14.

17. Gholizadeh, S., Halder, S. K., & Hampson, D. R. (2015). Expression of fragile X mental retardation protein in neurons and glia of the developing and adult mouse brain. Brain research, 1596, 22-30.

18. Hagerman, R. J., Berry-Kravis, E., Hazlett, H. C., Bailey, D. B., Moine, H., Kooy, R. F., Tassone, F., Gantois, I., Sonenberg, N., Mandel, J. L., & Hagerman, P. J. (2017). Fragile X syndrome. *Nature reviews Disease primers*, *3*(1), 1-19.

19. Hatton, D. D., Sideris, J., Skinner, M., Mankowski, J., Bailey Jr, D. B., Roberts, J., & Mirrett, P. (2006). Autistic behavior in children with fragile X syndrome: prevalence, stability, and the impact of FMRP. *American journal of medical genetics Part A*, *140*(17), 1804-1813.

20. Hébert, B., Pietropaolo, S., Même, S., Laudier, B., Laugeray, A., Doisne, N., Quartier, A., Lefeuvre, S., Got, L., Cahard, D., Laumonnier, F., E Crusio, W., Pichon, J., Menuet, A., Perche, O., & Briault, S. (2014). Rescue of fragile X syndrome phenotypes in Fmr1 KO mice by a BKCa channel opener molecule. Orphanet journal of rare diseases, 9(1), 1-10.

21. Higashimori, H., Schin, C. S., Chiang, M. S. R., Morel, L., Shoneye, T. A., Nelson, D. L., & Yang, Y. (2016). Selective deletion of astroglial FMRP dysregulates glutamate transporter GLT1 and contributes to fragile X syndrome phenotypes in vivo. Journal of Neuroscience, 36(27), 7079-7094.

22. Hodges, J. L., Yu, X., Gilmore, A., Bennett, H., Tjia, M., Perna, J. F., Chen, C. C., Li, X., Lu, J. & Zuo, Y. (2017). Astrocytic contributions to synaptic and learning abnormalities in a mouse model of fragile X syndrome. *Biological psychiatry*, *82*(2), 139-149.

23. Hodges, S. L., Nolan, S. O., Tomac, L. A., Muhammad, I. D., Binder, M. S., Taube, J. H., & Lugo, J. N. (2020). Lipopolysaccharide-induced inflammation leads to acute elevations in pro-inflammatory cytokine expression in a mouse model of Fragile X syndrome. *Physiology & Behavior*, *215*, 112776.

24. Jin, S. X., Higashimori, H., Schin, C., Tamashiro, A., Men, Y., Chiang, M. S. R., Jarvis, R., Cox, D., Feig, L., & Yang, Y. (2021). Astroglial FMRP modulates synaptic signaling and behavior phenotypes in FXS mouse model. GLIA, 69(3), 594–608.

25. Krasovska, V., & Doering, L. C. (2018). Regulation of IL-6 secretion by astrocytes via TLR4 in the fragile X mouse model. Frontiers in molecular neuroscience, 272.

26. Liao, L., Park, S. K., Xu, T., Vanderklish, P., & Yates, J. R. (2008). Quantitative proteomic analysis of primary neurons reveals diverse changes in synaptic protein content in fmr1 knockout mice. Proceedings of the National Academy of Sciences, 105(40), 15281-15286.

27. Maurin, T., Zongaro, S., & Bardoni, B. (2014). Fragile X Syndrome: from molecular pathology to therapy. *Neuroscience & Biobehavioral Reviews*, *46*, 242-255.

28. McLennan, Y., Polussa, J., Tassone, F., & Hagerman, R. (2011). Fragile x syndrome. *Current genomics*, *12*(3), 216-224.

29. Men, Y., Higashimori, H., Reynolds, K., Tu, L., Jarvis, R., & Yang, Y. (2022). Functionally clustered mRNAs are distinctly enriched at cortical astroglial processes and are preferentially affected by FMRP deficiency. *Journal of Neuroscience*.

30. Nikolic, L., Nobili, P., Shen, W., & Audinat, E. (2020). Role of astrocyte purinergic signaling in epilepsy. *Glia*, *68*(9), 1677-1691.

31. Oliveira, J. F., Sardinha, V. M., Guerra-Gomes, S., Araque, A., & Sousa, N. (2015). Do stars govern our actions? Astrocyte involvement in rodent behavior. Trends in neurosciences, 38(9), 535-549.

32. Pacey, L. K., & Doering, L. C. (2007). Developmental expression of FMRP in the astrocyte lineage: implications for fragile X syndrome. Glia, 55(15), 1601-1609.

33. Perche, F., Gosset, D., Mével, M., Miramon, M. L., Yaouanc, J. J., Pichon, C., Benvegnu, T., Jaffrés, P. A., & Midoux, P. (2011). Selective gene delivery in dendritic cells with mannosylated and histidylated lipopolyplexes. Journal of Drug Targeting, 19(5), 315-325.

34. Puchałowicz, K., Baranowska-Bosiacka, I., Dziedziejko, V., & Chlubek, D. (2015). Purinergic signaling and the functioning of the nervous system cells. *Cellular and Molecular Biology Letters*, *20*(5), 867-918.

35. Reynolds, K. E., Krasovska, V., & Scott, A. L. (2021b). Converging purinergic and immune signaling pathways drive IL-6 secretion by Fragile X cortical astrocytes via STAT3. Journal of Neuroimmunology, 361, 577745.

36. Reynolds, K. E., Wong, C. R., & Scott, A. L. (2021a). Astrocyte-mediated purinergic signaling is upregulated in a mouse model of Fragile X syndrome. Glia, 69(7), 1816-1832.

37. Richter, J. D., & Zhao, X. (2021). The molecular biology of FMRP: new insights into fragile X syndrome. *Nature Reviews Neuroscience*, *22*(4), 209-222.

38. Sabaratnam, M., Vroegop, P. G., & Gangadharan, S. K. (2001). Epilepsy and EEG findings in 18 males with fragile X syndrome. *Seizure*, *10*(1), 60-63.

39. Sarti, A. C., Vultaggio-Poma, V., Falzoni, S., Missiroli, S., Giuliani, A. L., Boldrini, P., Bonora, M., Faita, F., Di Lascio, N., Kusmic, C., Solini, A., Novello, S., Morari, M., Rossato, M., Wieckowski, M. R., Giorgi, C., Pinton, P., & Di Virgilio, F. (2021). Mitochondrial P2X7 receptor localization modulates energy metabolism enhancing physical performance. *Function*, *2*(2), zqab005.

40. Sitzmann, A. F., Hagelstrom, R. T., Tassone, F., Hagerman, R. J., & Butler, M. G. (2018). Rare FMR1 gene mutations causing fragile X syndrome: a review. *American Journal of Medical Genetics Part A*, *176*(1), 11-18.

41. Sluyter, R. (2017). The P2X7 receptor. *Protein reviews*, 17-53.

42. Smith, L. E., Barker, E. T., Seltzer, M. M., Abbeduto, L., & Greenberg, J. S. (2012). Behavioral phenotype of fragile X syndrome in adolescence and adulthood. *American journal on intellectual and developmental disabilities*, *117*(1), 1-17

43. Stefani, G., Fraser, C. E., Darnell, J. C., & Darnell, R. B. (2004). Fragile X mental retardation protein is associated with translating polyribosomes in neuronal cells. *Journal of Neuroscience*, *24*(33), 7272-7276.

44. Suzuki, A., Stern, S. A., Bozdagi, O., Huntley, G. W., Walker, R. H., Magistretti, P. J., & Alberini, C. M. (2011). Astrocyte-neuron lactate transport is required for long-term memory formation. Cell, 144(5), 810-823.

45. Van Snick, J. (1990). Interleukin-6: an overview. Annual review of immunology, 8(1), 253-278.

46. Wang, A. L., Liu, F., & Wang, G. (2014). Involvement of Voltage-Gated Ca2+ Channels in Autism Spectrum Disorders. North American Journal of Medicine and Science, 7(3).

47. Wang, H., Ku, L., Osterhout, D. J., Li, W., Ahmadian, A., Liang, Z., & Feng, Y. (2004). Developmentally-programmed FMRP expression in oligodendrocytes: a potential role of FMRP in regulating translation in oligodendroglia progenitors. Human molecular genetics, 13(1), 79-89.

48. Weiler, I. J., Irwin, S. A., Klintsova, A. Y., Spencer, C. M., Brazelton, A. D., Miyashiro, K., Comery, T. A., Patel, B., Ebervine, J., & Greenough, W. T. (1997). Fragile X mental retardation protein is translated near synapses in response to neurotransmitter activation. *Proceedings of the National Academy of Sciences*, *94*(10), 5395-5400.

49. Willemsen, R., & Kooy, F. (Eds.). (2017). Fragile X syndrome: from genetics to targeted treatment. Academic Press.

50. Yang, Q. Q., & Zhou, J. W. (2019). Neuroinflammation in the central nervous system: Symphony of glial cells. *Glia*, *67*(6), 1017-1035.

Links:

URL1: https://www.atcc.org/products/crl-2541 (18.05.2022.)

URL2: https://www.addgene.org/87929/ (11.06.2022.)

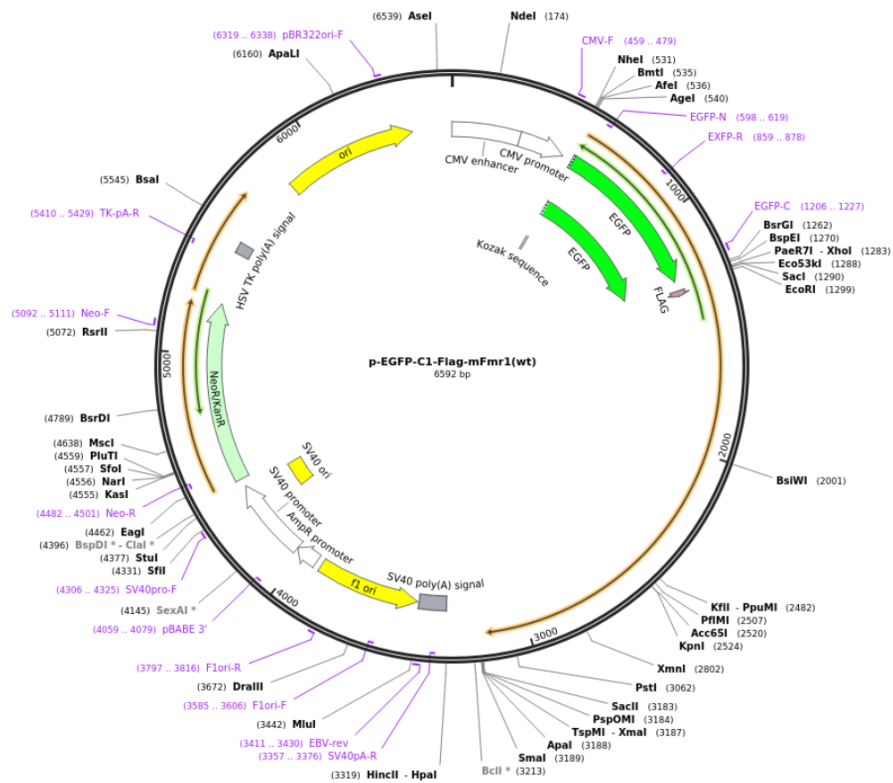# 6. ANNEXE

6.1. Plasmid maps
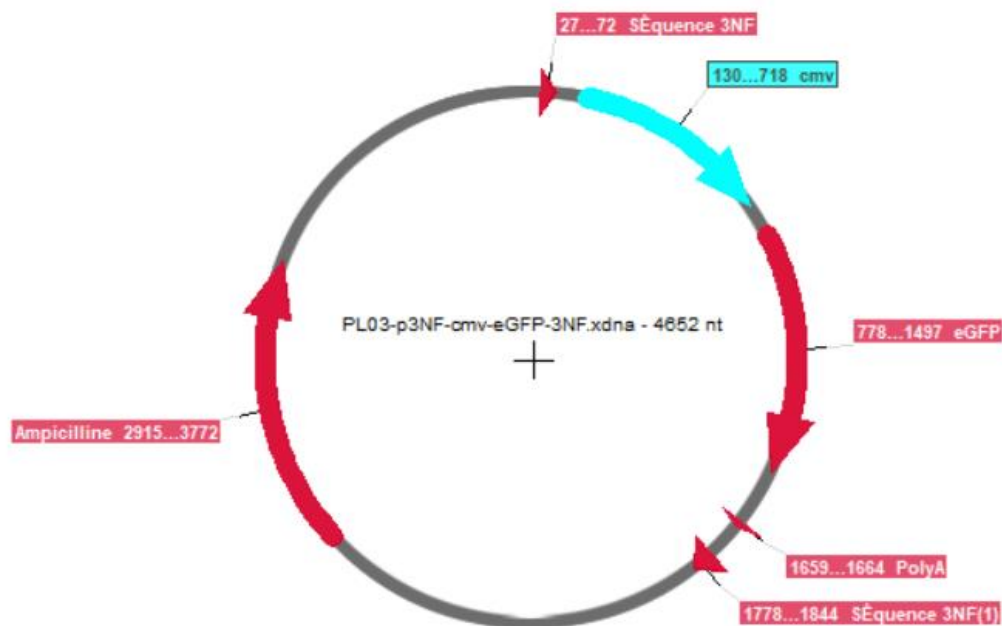

Figure 18. p-EGFP-C1-Flag-mFmr1 expression vector map (URL2).

Figure 19. PLO3-p3NF-cmv-eGFP-3NF expression vector map.